

APPLICATION OF DRIVING BEHAVIOR CONTROL SYSTEM USING ARTIFICIAL NEURAL NETWORK TO IMPROVE DRIVING COMFORT BY ADJUSTING AIR-TO-FUEL RATIO

ARIS TRIWIYATNO^{1*}, SUROTO MUNAHAR^{2,3}, M. MUNADI³
AND JOGA DHARMA SETIAWAN³

¹*Department of Electronics Engineering, Diponegoro University, Semarang, Indonesia*

²*Department of Automotive Engineering,*

Universitas Muhammadiyah Magelang, Magelang, Indonesia

³*Department of Mechanical Engineering, Diponegoro University, Semarang, Indonesia*

*Corresponding author: aristriwiyatno@elektro.undip.ac.id

(Received: 7 March 2023; Accepted: 22 May 2023; Published on-line: 4 July 2023)

ABSTRACT: Energy-efficient engines were introduced due to limited amount of global energy and the need for engine power to carry vehicle loads. It was discovered that the power factor of these engines was essential in developing automotive technology with subsequent significant effect on driving comfort. Moreover, it was possible to control the power and energy savings of vehicle engines by adjusting the Air to Fuel Ratio (AFR). Therefore, this study focused on achieving AFR values in the stoichiometric range of 14.7 in order to produce good emissions. The technology applied was observed to have some drawbacks, specifically in fulfilling engine power when the vehicle operates with a large load. This led to the development of a new method by designing an AFR control system with due consideration for driving behavior using an Artificial Neural Network (ANN). The aim was to overcome the problem of meeting engine power and ensuring better efficiency. The driving behavior was classified into through categories including the sporty, standard, and eco schemes. The eco scheme was the smooth behavior of a driver during the movement of the vehicle in a busy urban area, the sporty scheme was the responsive driving behavior when the vehicle operates on the highway at speeds above 80 km/h, and the standard scheme was the behavior between the eco and sporty schemes. Furthermore, the driving behavior in a sporty scheme required the addition of fuel to increase engine power while eco-scheme focused on reducing fuel to increase fuel economy. The findings showed that control system designed was able to improve driving comfort in terms of fuel economy during the eco scheme with an average AFR value of 15.68. The system further reduced the value to 13.66 during the sporty scheme. Furthermore, the AFR under stoichiometry was discovered to have produced the maximum engine power. The system was expected to be incorporated into electric, gas-fired and fuel cell vehicles in the future.

ABSTRAK: Faktor kuasa enjin dan enjin cekap tenaga adalah penting dalam membangunkan teknologi automotif. Mesin penjimat tenaga diperlukan kerana jumlah tenaga global yang terhad. Manakala kuasa enjin digunakan bagi membawa muatan kenderaan. Kedua-dua faktor ini sangat mempengaruhi keselesaan pemanduan. Penjimatan kuasa dan tenaga dalam enjin kenderaan boleh dipenuhi dengan mengawal Nisbah Angin kepada Minyak (AFR). Tumpuan kajian semasa adalah berorientasikan ke arah mencapai nilai AFR dalam julat stoikiometri (14.7) atas sebab ingin mencapai pelepasan terbaik. Namun begitu, teknologi ini mempunyai kelemahan terutama dalam

memenuhi kuasa enjin apabila kenderaan beroperasi dengan muatan besar. Oleh itu, kajian ini adalah berkaitan kaedah baharu bagi mengatasi masalah memenuhi kuasa enjin dan mencapai enjin cekap tenaga dengan mereka bentuk sistem kawalan AFR yang mempertimbangkan tingkah laku pemanduan menggunakan Rangkaian Neural Buatan (ANN). Tingkah laku pemanduan direka bentuk kepada tiga skim: sporty, standard dan eko. Skim eko adalah kelancaran tingkah laku pemandu apabila kenderaan bergerak di kawasan bandar yang sibuk. Skim sporty ialah tingkah laku pemanduan responsif apabila kenderaan beroperasi di lebuh raya pada kelajuan melebihi 80 km/j, dan skema standard ialah tingkah laku antara skim eko dan sporty. Tingkah laku pemanduan dalam skema sporty memerlukan penambahan bahan api bagi meningkatkan kuasa enjin. Sementara itu, tingkah laku pemanduan dalam skim eko memerlukan pengurangan bahan api bagi meningkatkan penjimatan bahan api. Hasil kajian menyatakan sistem kawalan yang direka mampu meningkatkan keselesaan pemanduan dari segi penjimatan bahan api apabila tingkah laku pemandu memasuki skim eko. AFR dicapai pada nilai purata 15.68. Apabila tingkah laku pemandu memasuki skim pemanduan sporty, sistem kawalan boleh mengurangkan AFR dengan nilai purata 13.66. AFR di bawah stoikiometri menghasilkan kuasa enjin maksimum. Pada masa hadapan, sistem ini berpotensi untuk dibangunkan pada kenderaan elektrik, menggunakan gas dan sel bahan api.

KEYWORDS: *driving behavior; AFR; ANN; engine power; fuel saving*

1. INTRODUCTION

Vehicle comfort is a very important topic in the development of automotive technology and it can be increased through suspension control [1], steering system power transfer, engine power, and fuel economy. It is also significantly related to the aspects of engine power and fuel economy, and these two concepts have become international issues presently focused on by world researchers [2] due to the limited energy problem [3,4] and the very significant increase in global energy consumption.

The current high increase in the number of vehicles using gasoline engines has made fuel-saving technology necessary. Meanwhile, there is also the need to have the appropriate engine power to move the vehicle, especially when it is carrying a heavy load. It is important to note that vehicle comfort can be achieved from the engine power and fuel economy aspects by controlling the Air to Fuel Ratio (AFR) which is categorized into three including lean mixture with AFR values above 14.7, ideal or stoichiometry ratio which is 14.7, and rich mixture with values below 14.7. The lean category usually produces low engine power with high fuel economy, the rich mixture is the opposite, and the stoichiometry category normally has optimal engine power and fuel economy.

Several studies have been conducted on AFR using different variables such as the application of fuzzy logic which is Artificial Intelligence (AI) to set AFR in a simulation [5]. It was discovered that the system was able to control the AFR with inaccurate signals or data but it has not been applied to real conduction. Another different study tried to add a variable turbo charge to increase the volumetric efficiency of the engine and changes were observed in the AFR because the turbo charge added forced air into the engine based on the power generated by the exhaust gas pressure [6]. However, the research has not yet integrated an intelligent control system to modify the AFR. Some studies have also started focusing on AFR stoichiometry control which was denoted by the achievement of lambda (λ) = 1 [7]. It is important to note that Lambda (λ) is a comparative value between the actual AFR and the stoichiometry of the theoretical AFR. This method also has some problems which are making the vehicle users complain, especially due to the low engine power when the vehicle is operating on a steep or inclined surface or carrying a large load.

Driving behavior has been empirically discovered to have a great influence on the fuel system (AFR) dynamics but it was discovered that no study has focused on controlling AFR through driving behavior. Previous studies have only focused on using several variables such as the development of a car using systems in autonomous vehicles, application of a simulation scale Connected Vehicle Driving Strategy with Intelligent Model (CVDS-IDM), design of safety systems on vehicles, analysis of driving behavior, vision technology or graphical display, and the vehicle emissions dynamics when at a traffic light.

Driving behavior in car-following has also been studied with several variations such as autonomous vehicle dynamics, the use of CVDS-IDM, and a safe car-following behavior system. Those related to the dynamics of the autonomous vehicle showed that the driver following a driverless autonomous vehicle was significantly affected psychologically [8]. Moreover, CVDS-IDM was defined as a simulator tool to predict driving behavior in real time by providing a driver a stimulus with various variables, especially when driving behind another vehicle [9]. It was discovered that the CVDS-IDM was able to model the car-following mechanism through the method applied by the driver. Another study also focused on safe driving behavior in order to develop a safety system based on the behavior of car-following drivers [10]. However, it was discovered that none of these three studies discuss the relationship between driving behavior and fuel consumption.

Further studies focused on driving behavior in relation to the safety systems design on vehicles such as the usage of cameras, vehicle theft prevention, and adaptive Forward Vehicle Collision Warning (FCW) systems [11] as well as the analysis of the driving behavior when the driver was sleepy [12]. The cameras were installed on the vehicle to record ongoing activities, hence it provides feedback for a sleepy driver in order to control the vehicle immediately and properly with the intention of reducing the occurrence of accidents. Martinelli [13] also prevented vehicle theft by comparing driving behavior against a database. The research was initiated by learning and storing the driver's behavior in a control system and was later compared with the pattern through which an individual drive. The engine of the vehicle was programmed to stop when the driving behavior stored and observed are not similar to protect the vehicle from theft. Another study by Yuan [14] used an adaptive Forward Vehicle Collision Warning (FCW) to avoid collisions when the driver is driving abnormally. This was achieved by detecting the distance between the vehicle and the monocular. It is important to note that all these studies did not also consider the relationship between fuel usage systems and driving behavior.

Scholars also researched the improvement of driving safety through several variables which include analyzing the attitude and performance of drivers during sudden braking or steering operations and determining their safety rating [15]. Another study also observed and assessed driver control and safe practices during the process of driving a vehicle using risky driving behavior as the research variable [16]. Moreover, Mafeni [17] and Takashi Bando [18] evaluated driving behavior errors with a focus on abnormal braking and vehicle speed operation when traveling at very high speeds. It was also observed that even though the studies have different objectives, none focused on energy consumption in evaluating driving behavior.

Subsequent research also focuses on driving behavior in autonomous and electric vehicles (EVs). This was observed from the design of a lateral system control based on autonomous vehicles by Hongbo [19] to trace the vehicle's turning angle accurately and provide a better steering control effect compared to conventional steering lateral control. Moreover, Ashkrof [20] developed EVs control strategies to select travel routes and determine battery charging locations based on driving behavior. These studies do not also discuss variables related to energy use.

An automatic control system was introduced to recognize driving behavior by Silver [21] and Yansong [22] to alert drivers when they exceed safety limits. Julian [23] also used vision sensors for the same purpose with the recognition results stored in a database and exclusively patented. These studies have interesting concepts but this could have been more exciting if the driving behavior recognition factor was used to control energy. Unfortunately, it was not included.

The other aspects studied in relation to driving behavior are traffic lights and graphical displays. This was observed in the analysis of emissions produced by vehicles at traffic lights, especially at road junctions, by Stagios [24] through the observations made about the changes in vehicle emissions on the highway due to driving behavior. It was discovered that it is possible to reduce emissions by up to 26% when the driver behaves in certain conditions. However, this study only focused on changes in emissions without considering the energy consumption factor in behavioral changes.

Kohl [25] also showed that graphic displays, especially images/messages that frequently appear, have a significant influence on safe driving behavior. It was discovered that the frequent graphic display reduces the focus of drivers while driving and this is very dangerous for safety. This is considered very interesting but this study did not include the energy control influenced by driving behavior. This was followed by studies conducted on the relationship between energy consumption and driving behavior. Xing [26] predicted future energy consumption by observing the behavior of the driver but the study does not lead to energy control.

This simply implies several variables have been considered in studying driving behavior such as car-following systems, CVDS-IDM simulations, vehicle safety systems design, driving behavior analysis, vision technology or graphical display, and the vehicle emissions dynamics at traffic lights. It has also been discovered from previous studies that fuel energy control can be denoted by AFR used to generate stoichiometry values, machine learning or artificial intelligence applications, and the use of turbochargers. However, research has not been conducted on using driving behavior to control fuel even though driving behavior has been empirically proven to have a significant influence on fuel consumption. Therefore, this research was used to discuss the application of a driving behavior system to control fuel using an Artificial Neural Network as a continuation of the previous study [26].

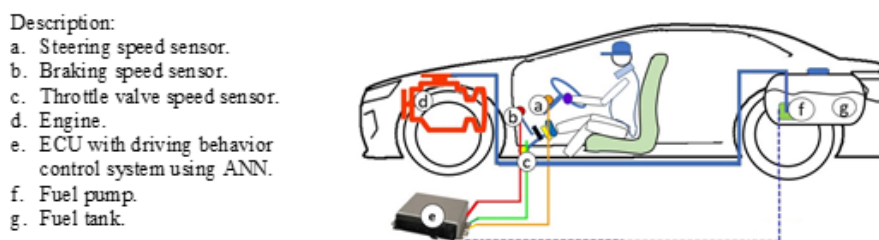


Fig. 1: The concept of the designed control system.

The control system developed based on the driving behavior using Artificial Neural Network (ANN) was successfully applied to real vehicles and presented in the following Figure 1. It was designed to work on three inputs which include the steering speed sensor (a), braking speed sensor (b), and throttle valve opening speed sensor (c) as well as supporting components to assist its performance which include an engine to generate power to drive the vehicle (d) and engine control unit – ECU (e) designed with ANN to recognize driving behavior in real time. The results obtained from the ANN were used to control fuel consumption through the fuel pump (f) placed in the fuel tank (g) in order to deliver fuel to the injectors. It is important to

note that the speed of the fuel pump was controlled by the ECU with the ANN applied to recognize driving behavior.

2. METHOD

2.1 Control System by Driving Behavior

The behaviors of drivers are usually different when driving based on their needs, mood, and inclinations, and this greatly influences vehicle operation and fuel consumption. This led to the design of three schemes to control the vehicle which include eco-driving, standard or stoichiometry, and sporty behaviors. The eco-driving is the behavior associated with vehicles operating smoothly on busy urban roads [27] and allows the driver to operate the throttle valve opening, braking, and steering smoothly at a speed of approximately 40-60 km/hour. The sporty scheme is a responsive driving behavior that involves the vehicle operating on a toll road [28] and the driver is expected to generally drive responsively at a vehicle speed of more or less than 80 km/hour. Meanwhile, the standard scheme is a driving behavior between the eco and sporty schemes.

Figure 2 shows the design of the control system developed in this study to regulate fuel using ANN with due consideration for the driving behavior. The ANN designed to be embedded in the control system is used to recognize driving behavior in real-time. Moreover, the algorithm method applied in the ANN was Levenberg Marquardt type learning (trainlm) while the learning performance was based on the Mean Squared Error (MSE) value using 300 nodes, one output layer, one hidden layer, and three inputs.

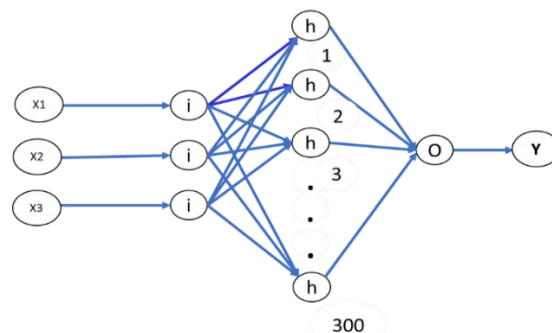


Fig. 2: ANN system design embedded in the control system.

The three ANN inputs consist of signals generated by the throttle valve opening speed sensor (X1), steering speed sensor (X2), and braking speed sensor (X3). These three sensors produce a speed signal which in the next process becomes the average acceleration value (MA) which is processed using Eqs. (1), (2), and (3). The ANN (Y) output is a driver behavior scheme to set the fuel pump.

The types of layers used include logsig, tansig, and purelin models while the number of neural network learning used was 20,000 epochs with a learning success rate of 99.93%. Furthermore, the neural network learning was conducted in the MATLAB Simulink software and later embedded in the control system (microcontroller mega 2560). This study uses 3285 data for ANN training. The training data used in this research is in the form of signal data generated by the throttle valve opening, steering, and braking sensors presented in Fig. 3. This training data is obtained from measurements of real driving behavior characteristics. Data from sensors is taken through data acquisition that has been processed beforehand using Eqs. (1), (2), and (3).

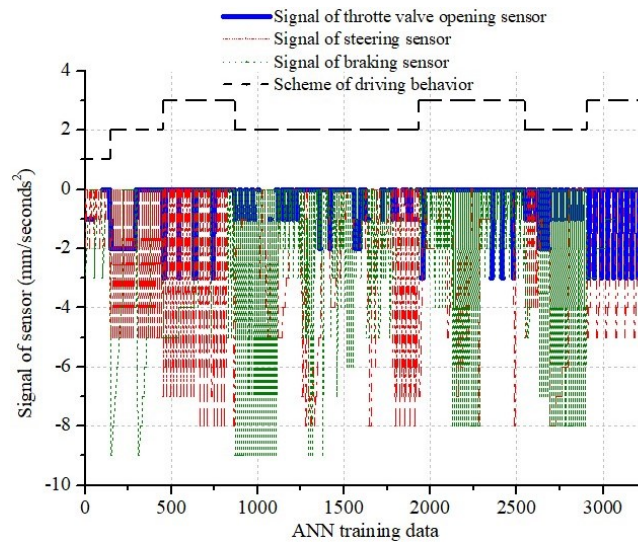


Fig. 3: Data used for ANN training.

Mapping driving behavior recognition with ANN has 27 levels. The driving behavior scheme was designed using the three schemes presented in Table 1. Driving behavior recognition mapping consists of three schemes, including eco-driving (A), stoichiometry/normal driving (B), and sporty driving (C) schemes. Determination of the driving behavior scheme serves to assess the characteristics of each driver. The detailed determination of the driving behavior scheme is presented in Table 4. Table 4 and it was discovered that it was designed on the operation of opening the throttle valve (X2), steering (X2), and braking (X3). The throttle valve opening operation has three low, medium, and high clusters for steering and braking operations. The findings of each cluster for throttle valve opening, steering and braking operations are presented in Table 3.

2.2 Equations Used in Control Systems

The throttle valve opening, steering, and braking sensors generated speed data which were later converted into an acceleration function embedded in the control system (Microcontroller Ni MyRio). Moreover, the average acceleration value (Moving Average - MA) was applied to analyze the driver's behavior from opening the throttle valve, steering, and braking. This method was preferred due to its ability to reduce the value of erratic variations [29,30], thereby increasing its suitability to recognize the variations in the driving behavior.

2.2.1 Acceleration Function Equation

The speed data generated by the throttle valve, steering, and braking sensors were converted to the acceleration function presented in Eq. (1).

$$a_i = \frac{(v_i - v_{(i-1)})}{(t_i - t_{(i-1)})} \quad (1)$$

where: $I = 1, 2, \dots, 180$

a_i = Acceleration value at the time I (mm/seconds²).

T = Time of speed change in seconds.

v_i = Speed value in period I (mm/seconds).

$v_{(i-1)}$ = Speed value in period $I - 1$ (mm/seconds).

The next process after the speed has been changed into an acceleration function with Eq. (1) was to determine the average acceleration value.

Table 1: Mapping driving behavior recognition with ANN system

No.	Schematic of driving behavior (Y)	Driving operation type		
		Opening of the throttle valve (X1)	Steering (X2)	Braking (X3)
1.	A	1	1	1
2.	B	1	1	2
3.	B	1	2	2
4.	B	1	1	3
5.	B	1	2	2
6.	B	2	2	2
7.	B	2	1	1
8.	B	2	2	1
9.	B	2	1	2
10.	C	3	1	1
11.	C	3	2	1
12.	C	3	1	2
13.	C	3	2	2
14.	C	3	2	3
15.	C	3	3	2
16.	C	3	3	3
17.	C	3	1	3
18.	C	3	3	1
19.	B	1	2	3
20.	B	1	3	2
21.	B	1	3	3
22.	B	1	3	1
23.	B	2	2	3
24.	B	2	3	3
25.	B	2	3	2
26.	B	2	3	1
27.	B	2	1	3

Description: 1 = low, 2= moderate, 3 = high, A= Eco driving scheme, B= Stoichiometry/standard driving scheme, C= Sporty driving scheme.

2.2.2 Calculation of Change in Average Acceleration

The acceleration value obtained from Eq. (1) was used to calculate the average value using the Moving Average (MA) method presented in Eq. (2).

$$MA_i = \frac{a_i + a_{i+1} + a_{i+2}}{3} \quad (2)$$

where:

$$i = 1, 2, \dots, 180$$

MA_i = Average acceleration (mm/seconds²).

a_i = Acceleration value in period i (mm/seconds²).

a_{i+1} = Acceleration value in period i+1 (mm/seconds²)

a_{i+2} = Acceleration value in period i+2 (mm/seconds²).

The MA value was successfully calculated using Eq. (2) while the average was calculated again using Eq. (3). It was discovered that the average MA had 178 constraints,

which were determined once every 15 minutes, and sent to the ECU to recognize driving behavior using the ANN embedded in the control system (microcontroller mega 2560).

$$\overline{MA} = \frac{MA_1 + MA_2 + \dots + MA_{178}}{178} \quad (3)$$

2.2.3 Control System Testing Set Up Developed

The control system test was designed by mounting an AFR sensor (1) on the exhaust gas line to detect the air and fuel mixture while a data acquisition microcontroller (2) was used to change the signal generated by the AFR sensor and the engine speed sensor (4). Moreover, the speed module (3) was employed to convert the pulse signal into a signal readable by the computer as indicated in Fig. 2. It was also observed that the control system (8) developed has two components which include a Ni MyRio microcontroller (a) and a control module (b) with a Mega 2560 microcontroller and an electronic circuit.

The speed data generated every 5 seconds by the throttle valve opening, braking, and steering speed sensors were converted into an acceleration function in the Ni MyRio Microcontroller (a). Moreover, the process to change the speed function into an acceleration function is presented in Eq. (1) after which the acceleration data obtained were averaged through Eq. (2) using the Moving Average – MA method. The MA average results were also calculated using Equation (3) every 15 minutes and sent to the ECU where an AI system with a neural network was used to perform clustering, analyze the different kinds of driving behavior, and send the cluster results to the speed controller module. The speed controller module was applied to control the fuel pump (2) to ensure the fuel is supplied to the engine according to the driving behavior. Additionally, an AI system with a neural network is embedded in the Mega 2560 microcontroller. The control system application setup is presented in Fig. 4.

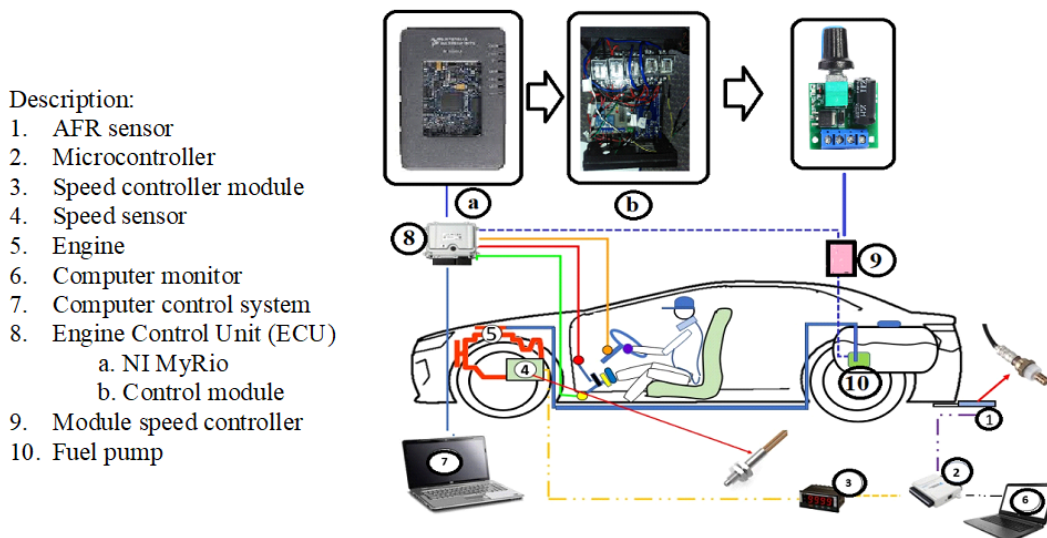


Fig. 4: Driving behavior control system test setup.

The installation of equipment to test the control system with driving behavior is presented in Fig. 5. The AFR sensor was used to measure the air and fuel mixture, the throttle valve speed sensor was mounted on one shaft with the throttle position sensor, while the braking speed sensor was fixed on the brake master shaft and actuated by the brake pedal. Moreover, the steering speed sensor was placed on the side of the steering shaft using a V belt. It is important to note that there was direct documentation of the behavioral recognition test while the speed sensor was used to measure engine speed. While the specifications of the equipment used in the study are presented in Table 2.

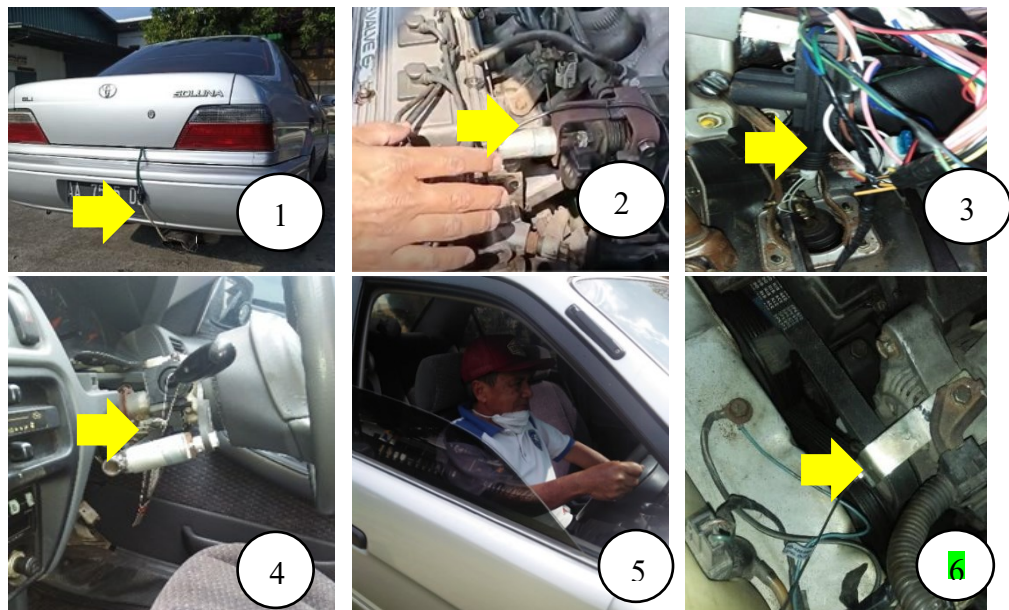


Fig. 5: Installation of AFR sensor (1), throttle valve speed sensor (2), braking speed sensor (3), steering speed sensor (4), driving operation (5), and engine speed sensor (6).

The installation of equipment to test the control system with driving behavior is presented in Fig. 5. The AFR sensor was used to measure the air and fuel mixture, the throttle valve speed sensor was mounted on one shaft with the throttle position sensor, while the braking speed sensor was fixed on the brake master shaft and actuated by the brake pedal. Moreover, the steering speed sensor was placed on the side of the steering shaft using a V belt. It is important to note that there was direct documentation of the behavioral recognition test while the speed sensor was used to measure engine speed. While the specifications of the equipment used in the study are presented in Table 2.

Table 2: Specifications of the equipment used

No.	Description	Specification
a.	Steering speed sensor	12-volt Direct Current (DC) motor with gear ratio and dimensions of $\varnothing 30 \times 60$ mm.
b.	Braking speed sensor.	
c.	Throttle valve speed sensor.	
d.	Engine.	Gasoline engine with injection type, which has a volume of 1500 cc.
e.	ECU with driving behavior control system using ANN.	NI MyRIO microcontroller and speed controller module equipped with atmega 2560 microcontroller.
f.	Fuel pump	12-volt DC rotary type
g.	Fuel tank	Capacity 44 liters
h.	Test vehicle	Saloon-type vehicle with a capacity of 4 passengers

3. RESULTS AND DISCUSSION

3.1 Throttle Valve Opening Sensor Results

The control system designed was applied directly to assess driving behaviors in order to determine the characteristics of drivers in real time based on three schemes which include the eco, stoichiometry/standard, and sporty schemes. Each of these schemes was determined using the changes in acceleration generated by the throttle valve opening, steering, and

braking sensors as the input. Moreover, the throttle valve opening signal was calculated through four stages which include the measurement of the throttle valve opening speed, change of the speed to acceleration, calculation of the Moving Average (MA) value, and determination of the average MA.

The change in the throttle valve opening speed was monitored over three periods as indicated in Fig. 6 with the first period found to be between 0 - 900 seconds, the second was 901-1800 seconds, and the third was 1,801 – 2,700 seconds. The findings showed that the speed change for these periods was 0–2.5, 0–2.6, and 0–4.6 mm/second respectively. It was observed that the third period tends to have a higher speed change rate and density level.

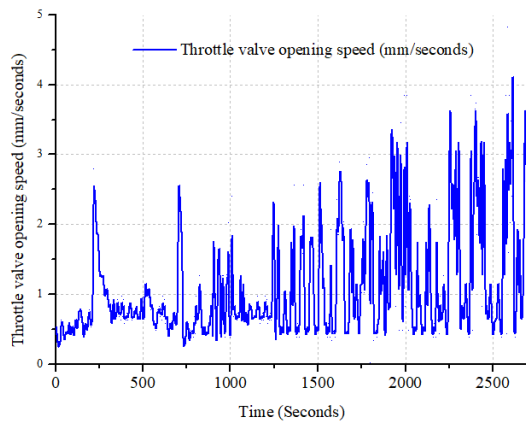


Fig. 6: Change of throttle valve opening speed.

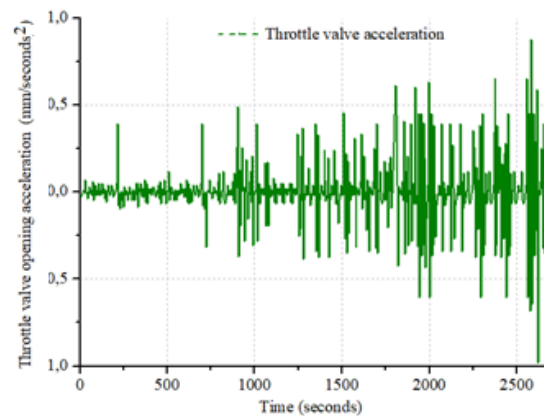


Fig. 7: Change of throttle valve opening acceleration.

The speed data presented in Fig. 6 was converted into an acceleration function using Eq. (1) and the results are presented in Fig. 7 as a function of the change in acceleration. It was discovered that there was an acceleration value of 0 – 0.5 mm/seconds² and a negative acceleration or deceleration value of 0-(-0.45 mm/seconds²) for 0 – 900 seconds. The findings also showed that the second period, 901 – 1,800 seconds, had 0 – 0.7 mm/seconds² and 0-(-0.7 mm/seconds²) while the third period, 1,801 – 2,700 seconds, had 0 – 0.9 mm/seconds² and 0-(-0.9 mm/seconds²) respectively. However, it is important to note that the third period had a higher density.

The acceleration/deceleration values presented in Fig. 7 were used in the next process to determine the average using the MA method in Eq. (2). This was also followed by finding the average of the MA values using Eq. (3) and the results are presented in Fig. 8. It was discovered that the MA value for the 0 – 900 seconds period ranged from 0 – 0.14 mm/seconds² and a negative acceleration (deceleration) value of 0-(-0.14 mm/seconds²). The results further showed that the 901 – 1,800 seconds period had 0 – 0.12 mm/seconds² and 0-(-0.12 mm/seconds²) while 1,801 – 2,700 seconds period had 0 – 0.2 mm/seconds² and 0-(-0.22 mm/seconds²) respectively. Meanwhile, the average MA for 0 – 900 seconds was found to be 0.00 while 901 – 1,800 seconds had 0.002, and 1801 – 2700 seconds had 0.003. It is pertinent to restate that the average MA value was determined every 15 minutes and sent to the developed control system. It was discovered that the highest MA average value was recorded in the last period.

3.2 Steering Sensor Results

The changes observed in the steering speed of each driver are presented in Fig. 9. It was discovered that the drivers possess quite diverse characteristics as observed with the 0

– 17 mm/second recorded for the 0 – 900 seconds period, 0 – 14 mm/seconds for the 901 – 1,800 seconds period, and 0 – 43 mm/seconds for the 1,801 – 2,700 seconds period which is the highest compared to the others.

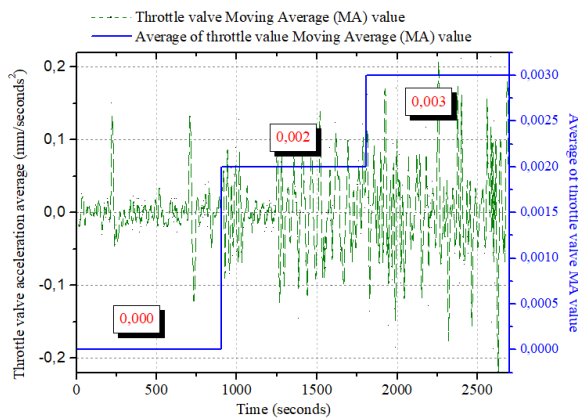


Fig. 8: Average MA value of driver throttle valve opening behavior.

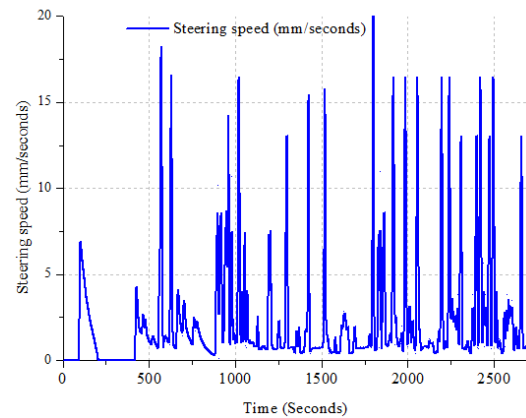


Fig. 9: Steering speed changes behavior.

The change in driver acceleration presented in Fig. 10 showed that the 0 - 900 seconds period had an acceleration value of 0 – 4 mm/seconds² and a negative acceleration (deceleration) value of 0-(-4 mm/seconds²) while 901 – 1,800 seconds period had 0 – 4.1 mm/seconds² and 0-(-4.1 mm/seconds²) and 1,801 – 2,700 seconds period had 0 – 5.8 mm/seconds² and 0-(-3 mm/seconds²) respectively. It was observed that the driver tends to add more steering acceleration in the third period.

The MA values recorded based on the changes in the driver's steering acceleration are presented in Fig. 11. It was discovered that the 0 – 900 seconds period had an MA range between 0 - 1.3 mm/seconds² and negative acceleration (deceleration) of 0-(-1.3 mm/seconds²) while the 901 – 1,800 seconds period had 0 – 1.1 mm/seconds² and 0-(-1.1 mm/seconds²) and the 1,801 – 2,700 seconds period had 0 – 1.1 mm/seconds² and 0-(-1.1 mm/seconds²) respectively. Moreover, the average MA value in the 0 – 900 seconds period was found to be 0.0000, the 901 – 1,800 seconds period had 0.002, and the 1,801 – 2,700 seconds had 0.03 which is the highest.

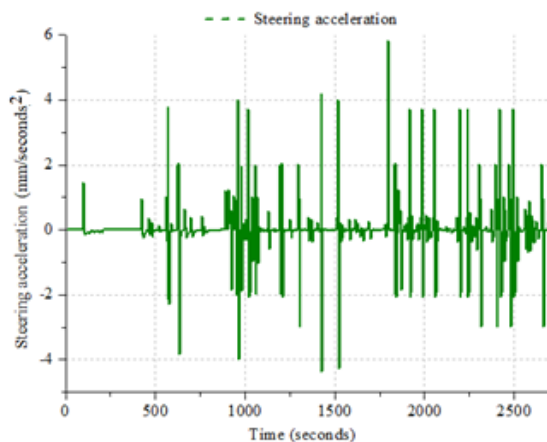


Fig. 10: Changes in steering acceleration behavior while driving.

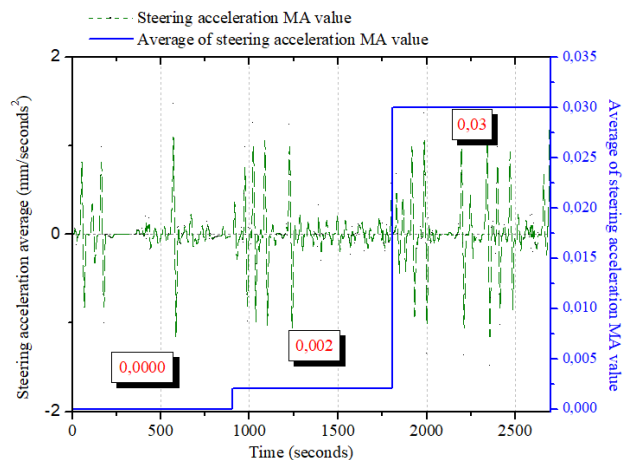


Fig. 11: Average MA value of driver steering behavior.

3.3 Braking Sensor Results

The changes in the driver's braking speed presented in Fig. 12 showed that the value at the 0 – 900 seconds period was 0–2.9 mm/second, the 901 – 1,800 seconds period had 0–2.6 mm/second, and the 1,801 – 2,700 seconds had 0 – 4.5 mm/second. This implies the 0 – 900 seconds period has the greatest braking speed and lower density frequency compared to the others.

The speed data presented in Fig. 10 were converted into an acceleration function through Eq. (1) to determine the changes in driver acceleration and the results are presented in Fig. 13. It was discovered that the pattern acceleration for the drivers at the 0 – 900 seconds period was in the range of 0 – 0.4 mm/seconds² and a negative acceleration (deceleration) value of 0–(-0.3 mm/seconds²) while the 901 – 1,800 seconds period had 0 – 0.7 mm/seconds² and 0–(-0.6 mm/seconds²) and 1,801 – 2,700 seconds period had 0 – 0.8 mm/seconds² and 0–(-0.8 mm/seconds²) respectively.

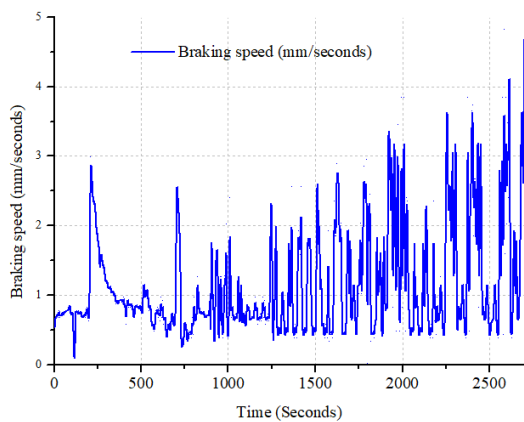


Fig. 12: Braking speed on observed driving behavior.

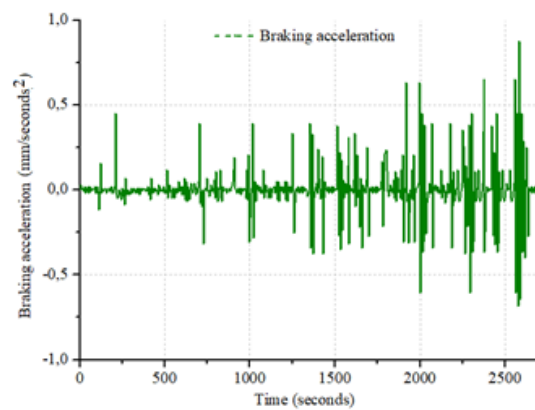


Fig. 13: Changes in the acceleration of the driver's braking behavior.

The MA values associated with the changes in the driver's braking acceleration are presented in Fig. 14. It was discovered that the 0 – 900 seconds period has a pattern where the MA values had the lowest frequency with values ranging between 0 – 0.15 mm/seconds² and negative acceleration (deceleration) values 0–(- 0.13 mm/seconds²). The findings further showed that the 901 – 1,800 seconds period had 0 – 0.12 mm/seconds² and 0–(-0.12 mm/seconds²) while the 1,801 – 2,700 seconds period had 0 – 2.1 mm/seconds² and 0–(-0.18 mm/seconds²). These MA values were later used to determine the average MA and the results showed that the value for the second driver was 0.0003 for the 0 – 900 seconds period, 0.0016 for the 901 – 1,800 seconds period, and 0.0021 for the 1,801 – 2,700 seconds period. This implies the 0 – 900 seconds period has the lowest average MA.

3.4 Driving Behavior Recognition Range

The driving behavior control system was designed using several variables that cause a slight difference between the simulated conditions and the real control system. It was discovered from the control system that the real driving behavior has a negative value because of the deceleration process and this cannot be read by the microcontroller. Therefore, a normalization system was needed through the inclusion of several different variables in the simulation scale and real control systems but the concept remains the same. Normalization is a process of adding constants to signal conditioning so that the microcontroller can work according to its designation. The methods used to recognize the

driving behavior are listed in Table 3 while the real decision-making process using the control system designed was based on the cluster system developed with the average MA value as indicated in Table 4.

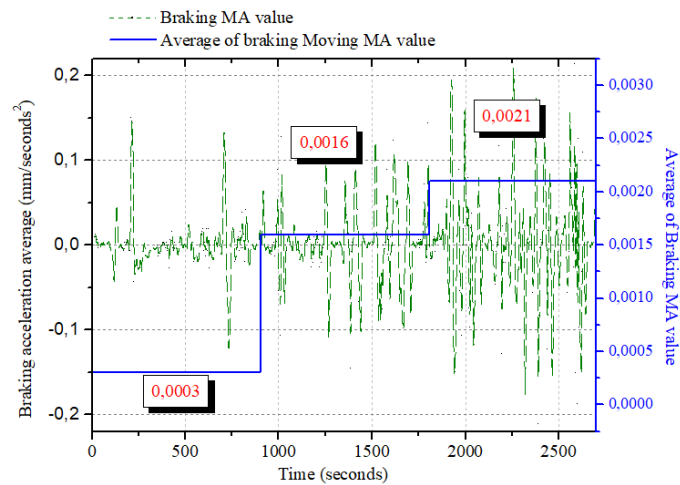


Fig. 14: Average MA value of the driver's braking behavior.

Table 3: Cluster average (\overline{MA}) for the throttle valve, steering, and braking

Description	Low (mm/seconds ²)	Middle (mm/seconds ²)	High (mm/seconds ²)
MA throttle valve acceleration	(-0.001)-0.001	0.002	0.003
MA from steering	(-0.02) - 0.02	(-0.05) – (-0.03) & 0.03 - 0.05	(-0.08) – (-0.06) & 0.06 - 0.08
MA of braking acceleration	(-0.0003)-0.0003	(-0.0009)–(-0.0006) & 0.0006 - 0.0009	(-0.005) – (-0.001) & 0.001 - 0.005

The average MA value generated by the sensor was analyzed to identify and recognize the driving behavior clusters using the ANN that has been trained and embedded in the controller system as presented in Table 3. It was discovered that the first period was in the eco scheme, the second period was in the stoichiometric scheme, and the third period was in the sporty scheme.

Table 4: Recognition of the driver's steering behavior in the control system

Description	First period (0-900s)	Second period (901-1,800s)	Third period (1801-2,700s)
MA throttle valve acceleration	Low (0.000)	Middle (0.002)	High (0.003)
MA acceleration steering	Low (0.0088)	Low (0.0101)	Low (0.0021)
MA braking acceleration	Low (0.0003)	High (0.0016)	High (0.0021)
Driving behavior scheme	<i>Eco</i>	<i>Stoichiometry</i>	<i>Sporty</i>

3.5 AFR Dynamics Results

The AFR values were measured using the data previously acquired and validated through an AFR meter and were subsequently applied to determine the influence of driving behavior on their variations based on the information in Table 3. The first period is in the eco scheme, the second is in the stoichiometric scheme, and the third is in the sporty scheme. It is important to note that vehicles experience acceleration and deceleration when operating on the highway. Acceleration is a condition associated with an increase in the speed of the vehicle by opening the throttle valve while deceleration involves reducing the vehicle's speed by closing the throttle valve. An increase in the vehicle speed by opening the throttle valve usually leads to a decrease in the AFR value and vice versa. The dynamics of the AFR value including the increase or decrease are presented in Figure 15 for the models with and without the driving behavior control system.

In the application of the driving behavior control system, the first period of driving behavior is known to have an AFR value between 14.8 – 17.7 with an average of 15.87, while the second period is between 14 – 16.6 with an average of 14.84, and the third period had the value is between 11.5 – 16 and the average is 13.66. This shows that the driving behavior in the first period allowed maximum fuel economy compared to the second and third periods. Meanwhile, the driving behavior in the third period led to the production of maximum power by the engine as indicated by the average AFR value recorded. Meanwhile, the dynamics of AFR without applying a driving behavior control system have quite a high difference in average values. The average AFR value without the developed control system is 14.78 for 2700 seconds. In the first period, the driver rarely decelerates, so the AFR value has a lower fluctuation range value when compared to the second and third periods.

The achievement of the highest fuel economy through the AFR value above the stoichiometry of 14.7. This is in line with a previous study that predicted the potential development of technology to achieve a lean AFR scale above the stoichiometry for commercialization purpose in order to have energy-efficient machines [31]. The research did not discuss the exact conditions to implement lean AFR but this current study considered its application based on driving behavior. It was discovered that the AFR above stoichiometry achieved in the first period, 0 – 900 seconds, led to smoother acceleration and this implies there is no need for large engine power.

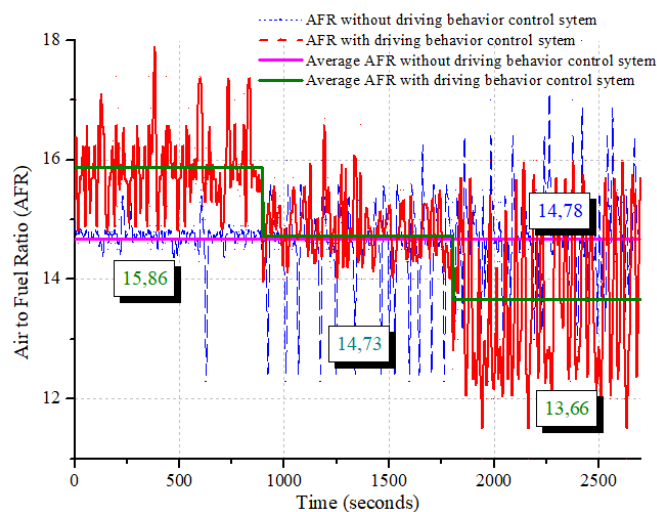


Fig. 15: AFR dynamics on observed driving behavior.

The AFR values in the second period, 901 – 1,800 seconds, are classified to be in the stoichiometric range (14.7) and this is in line with the findings of a previous study that AFR stoichiometry ensures the achievement of the most optimal value for power and fuel saving [7,32]. The research did not discuss the time and requirements to achieve maximum power saving but these are developed in this current study based on driving behavior.

The driving behavior in the third period, 1,801 – 2,700 seconds, was observed to have led to the fulfillment of maximum power as indicated by the average AFR stoichiometry value of 13.66. This agrees with the findings of a previous study that an AFR under a stoichiometry value of 12–14 usually produces the greatest engine power [33]. The control system showed that the driving behavior required high engine power and this led to the addition of more fuel at an average AFR value of 13.66.

This shows that the control system was successfully developed with due consideration for the driving behavior. This was able to improve driving comfort in terms of fuel economy as indicated by the AFR values above stoichiometry and fulfillment of the engine power requirements with values below stoichiometry. It was discovered that the fuel economy was satisfied in the first period when driving behavior is categorized as eco-scheme while the demand for the engine power was fulfilled in the third period when driving behavior is included in the sporty scheme.

4. CONCLUSION

The design of AFR management with driving behavior control using ANN has been successfully applied to actual vehicles. The designed control system can recognize driver behavior in real-time to control fuel and increase vehicle comfort. Driving comfort is achieved by meeting the need for fuel economy when the driving behavior is included in the eco-driving scheme and aspects of fulfilling engine power when the driving behavior is included in the sporty scheme. When the driver enters the eco-driving scheme, the control system can control AFR with an average value of 15.68 (entering the lean range). AFR above stoichiometry can improve fuel economy. The eco scheme is achieved in the first period (0–900 seconds), where this decision is based on the MA value of throttle valve acceleration in the low category (0.0000 mm/second²), MA steering acceleration in the low category (0.0088 mm/second²) and braking acceleration MA in the category low (0.0003 mm/s²). When the driving behavior enters the sporty driving scheme, the control system can control AFR with an average value of 13.66 (below stoichiometry). AFR under stoichiometry produces maximum engine power. The sporty scheme is achieved in the third period (0–900 seconds), where this decision is based on the MA value of throttle valve acceleration in the high category (0.003 mm/second²), MA steering acceleration in the low category (0.0021 mm/second²) and braking acceleration MA in the high category (0.0021 mm/second²). This research is applied to vehicles with gasoline engines and has not considered the road angle. For this reason, future research can be applied to electric, gas-fueled, and fuel-cell vehicles, considering the road angle.

ACKNOWLEDGMENT

The authors are grateful to the Diponegoro University and the Universitas Muhammadiyah Magelang for supporting this research.

REFERENCES

- [1] Burdzik R. (2022) A comprehensive diagnostic system for vehicle suspensions based on a neural classifier and wavelet resonance estimators. *Measurement*, 200: 111602
<https://doi.org/10.1016/j.measurement.2022.111602>.
- [2] Uslu S, Celik MB.(2020) Performance and exhaust emission prediction of a si engine fueled with i amyl alcohol-gasoline blends : An ANN coupled RSM based optimization. *Fuel*, 265: 116922. <https://doi.org/10.1016/j.fuel.2019.116922>.
- [3] Al-fattah SM. (2020) Non-OPEC conventional oil : Production decline, supply outlook and key implications. *Journal of Petroleum Science and Engineering* 189: 107049.
<https://doi.org/10.1016/j.petrol.2020.107049>.
- [4] Kutlu O. (2020) Global oil production declines in June 2020. *Energy*. Available:
<https://www.-aa.com.tr/en/energy/international-organization/global-oil-production-declines-in-june-2020-/29901>.
- [5] Wang Y, Fan Y, Wang D, Liu Y, Qiu Z, Liu J. (2020) Optimization of the areas of solar collectors and photovoltaic panels in liquid desiccant air-conditioning systems using solar energy in isolated low-latitude islands. *Energy*, 198: 117324.
<https://doi.org/10.1016/j.energy.-2020.117324>.
- [6] Gagliardi G, Mari D, Tedesco F, Casavola A. (2021) An Air-to-Fuel ratio estimation strategy for turbocharged spark-ignition engines based on sparse binary HEGO sensor measures and hybrid linear observers. *Control Engineering Practice*, 107: 104694.
[doi:10.1016/j.conengprac.2020.104694](https://doi.org/10.1016/j.conengprac.2020.104694).
- [7] Ahmed SFA. (2019) Analyzing and predicting the relation between air – fuel ratio (AFR), lambda (λ) and the exhaust emissions percentages and values of gasoline - fueled vehicles using versatile and portable emissions measurement system tool. *SN Applied Science*, 1(11): 1-12. <https://doi.org/10.1007/s42452-019-1392-5>.
- [8] Zhao X, Wang Z, Xu Z, Wang Y, Li X, Qu X. (2020) Field experiments on longitudinal characteristics of human driver behavior following an autonomous vehicle. *Transportation Research Part C: Emerging Technologies*, 114: 205-224.
<https://doi.org/10.1016/j.trc.2020.02.018>.
- [9] Sharma A, Zheng Z, Bhaskar A, Haque M. (2019) Modelling car-following behaviour of connected vehicles with a focus on driver compliance. *Transportation Research Part B*, 126: 256-279. <https://doi.org/10.1016/j.trb.2019.06.008>.
- [10] Fadhloun K, Rakha H. (2020) Novel vehicle dynamics and human behavior car-following model : Model development and preliminary testing. *International Journal of Transportation Science and Technology*, 9: 14-28. <https://doi.org/10.1016/j.ijst.2019.05.004>.
- [11] Grove K, Soccolich S, Engström J, Hanowski R. (2019) Driver visual behavior while using adaptive cruise control on commercial motor vehicles. *Transportation Research Part F*, 60: 343-352. <https://doi.org/10.1016/j.trf.2018.10.013>.
- [12] Fung KC, Dick TJ.(2016) System and method for responding to driver behavior.
<https://patents.google.com/patent/US9440646B2>.
- [13] Martinelli F, Mercaldo F, Orlando A, Nardone V, Santone A, Kumar A. (2020) Human behavior characterization for driving style recognition in vehicle system. *Computers & Electrical Engineering*, 83: 02504. <https://doi.org/10.1016/j.compeleceng.2017>.
- [14] Yuan Y, Lu Y, Wang Q. (2020) Adaptive forward vehicle collision warning based on driving behavior. *Neurocomputing*, 408: 64-71. <https://doi.org/10.1016/j.neucom.2019.11.02>.
- [15] Raz O, Fleishman H, Mulchadsky I. (2008) System and method for vehicle driver behavior analysis and evaluation. <https://patents.google.com/patent/US7389178B/en>.
- [16] Hong Z, Chen Y, Wu Y. (2020) A driver behavior assessment and recommendation system for connected vehicles to prod Prevention, 139: 105460.
<https://doi.org/10.1016/j.aap.2020.-105460>.
- [17] Mafeni J, Majid S, Mesgarpour M, Torres M, Figueredo GP, Chapman P. (2020) Evaluating the impact of Heavy Goods Vehicle driver monitoring and coaching to reduce risky behaviour, *Accident Analysis & Prevention*, 146: 105754.
<https://doi.org/10.1016/j.aap.2020.105754>.

- [18] Bando T. (2015) System for detecting abnormal driving behavior. <https://patents.google.com-/patent/US9111400B2/en>.
- [19] Hongbo G, Guotao X, Hongzhe L, Xinyu Z. (2017) Lateral control of autonomous vehicles based on learning driver behavior via cloud model. *The Journal of China Universities of Posts and Telecommunications*, 24(2): 10-17. [http://dx.doi.org/10.1016/S1005-8885\(17\)601](http://dx.doi.org/10.1016/S1005-8885(17)601).
- [20] Ashkrof P, Homem G, Correia DA, Van Arem B. (2020) Analysis of the effect of charging needs on battery electric vehicle drivers' route choice behaviour : A case study in the Netherlands. *Transportation Research Part D*, 78: 102206. <https://doi.org/10.1016/j.trd.2019.-102206>.
- [21] Silver A, Lewis L. (2015) Automatic identification of a vehicle driver based on driving behavior. <https://patents.google.com/patent/US9201932B2/en>.
- [22] Yansong R, O'Gorman L, Wood TL. (2019) Driver behavior monitoring systems and methods for driver behavior monitoring. <https://patents.google.com/patent/US9201932B2/en>.
- [23] Julian DJ and Agrawal A. (2017) Driver behavior monitoring. <https://patents.google.com-/patent/US10460600B2/en>.
- [24] Stogios C, Kasraian D, Roorda MJ, and Hatzopoulou M. (2019) Simulating impacts of automated driving behavior and traffic conditions on vehicle emissions. *Transportation Research Part D*, 76: 176-192. <https://doi.org/10.1016/j.trd.2019.09.020>.
- [25] Kohl J, Gross A, Henning M, Baumgarten T. (2020) Driver glance behavior towards displayed images on in-vehicle information systems under real driving conditions. *Transportation Research Part F: Traffic Psychology and Behaviour*, 70: 163-174. <https://doi.org/10.1016/j.trf.2020.01.017>.
- [26] Xing Y, Lv C, Cao D, Lu C. (2020) Energy oriented driving behavior analysis and personalized prediction of vehicle states with joint time series modeling. *Applied Energy*, 261: 114471. <https://doi.org/10.1016/j.apenergy.2019.114>.
- [27] Vaezipour A, Rakotonirainy A, Haworth N. (2018) A simulator evaluation of in-vehicle human machine interfaces for eco-safe driving. *Transportation Research Part A: Policy and Practice*, 118: 696-713. <https://doi.org/10.1016/j.tra.2018.10.022>.
- [28] Reinolsmann N, Alhajyaseen W, Brijs T, Pirdavani A, Hussain Q, Brijs K. (2019) Investigating the impact of dynamic merge control strategies on driving behavior on rural and urban expressways – A driving simulator study. *Transportation Research Part F: Traffic Psychology and Behaviour*, 65: 469-484. <https://doi.org/10.1016/j.trf.2019.08.010>.
- [29] Kiat D, Poh H, Yee C, Zhen R, Markus C, Ping T. (2021) Internal quality control : Moving average algorithms outperform westgard rules. *Clinical Biochemistry*, 98: 63–69. <https://doi.org/10.1016/j.clinbiochem.2021.09.007>.
- [30] Maverick JB. (2022) Advantages and disadvantages of the Simple Moving Average (SMA)?, Investopedia. Available: <https://www.investopedia.com/ask/answers/013015/what-are-main-advantages-and-disadvantages-using-simple-moving-average-sma.asp>. [Accessed: 05-May-2022].
- [31] Zhu C, Wang P, Wang P, Liu Z, Wang P, Liu Z. (2018) Model Prediction Control of Fuel-Air Ratio for Lean-Burn Spark Ignition Gasoline. *IFAC-PapersOnLine*, 51(31): 640–645. <https://doi.org/10.1016/j.ifacol.2018.10.150>.
- [32] Sardarmehni T, Aghili AA, Menhaj MB. (2019) Fuzzy model predictive control of normalized air-to-fuel ratio in internal combustion engines. *Soft Computing*, 23(15): 6169-6182. <https://doi.org/10.1007/s00500-018-3270>, 2019.
- [33] Martyr A and Plint M. (2007) Third Edition Engine Testing Theory and Practice. Elsevier Ltd.